Journal of
Engineering Sciences
Faculty of Engineering
Assiut University
JES
مجلة
العلوم الهندسية
كلية الهندسة
جامعة أسيوط
journal homepage: http://jesaun.journals.ekb.eg

Comparative Effects of Carbon Fiber Reinforcement on Polypropylene and Polylactic Acid Composites in Fused Deposition Modeling.

Received 6 November 2024; Revised 24 December 2024; Accepted 24 December 2024

Alhassan Abdelhafeez[1]
Yasser Abdelrahman[2]
M-Emad S. Soliman [3]
Shemy M. Ahmed [4]

Keywords
Carbon-fiber reinforced plastic, Fused deposition modeling, Mechanical properties, Hydrophilicity, Gaussian process regression

Abstract: This study offers a comparative evaluation of the impact of carbon fibre reinforcement on polypropylene (PP) and polylactic acid (PLA) matrices, focusing on their application in fused deposition modelling (FDM). Composite filaments with varying micro carbon fibre (MCF) contents were fabricated for both matrices, with their mechanical, moisture absorption, and morphological properties thoroughly characterized. In PP composites, MCF addition significantly improved tensile and flexural strengths, achieving optimal enhancement at 9.09 wt%, where tensile and flexural strengths rose by 75% and 100%, respectively, compared to pure PP. Conversely, PLA composites showed slight strength increases at lower MCF contents (below 5 wt %) but experienced strength reductions as fibre content exceeded this threshold. However, both materials exhibited increased stiffness (elastic modulus) with rising MCF levels, though PLA achieved optimal strength at a lower fibre loading. Moisture absorption increased in both matrices as fibre content rose; PP showed a proportional increase, whereas PLA displayed more pronounced absorption due to inter- and intra-filament porosities. Optical microscopy (OM) highlighted further differences: PP retained fibre distribution and bonding over a wide range of MCF levels, while PLA showed strong fibre adhesion and ductile fracture behaviour at lower MCF, shifting to brittle fracture and void formation at higher levels. Gaussian Process Regression (GPR) modelling corroborated these trends, identifying optimal MCF content as 9.09 wt% for PP and around 2.5 wt% for PLA. These findings provide guidance on selecting material and fibre loading for FDM applications, with each material achieving a unique balance of mechanical performance and moisture resistance.

1. Introduction

Additive manufacturing, commonly referred to as 3D printing, has revolutionized production techniques across various industries by enabling the creation of complex structures layer by layer from digital models. Among the prominent methods in 3D printing is Fused Deposition Modeling

[1]Mechanical Design and Production Engineering Dept., Faculty of Engineering, Assiut University, Assiut, Egypt. alhassan_m.abdelhafeez@eng.aun.edu.eg
[2] Mechanical and Industrial Engineering Dept., College of Engineering, Majmaah University, Al Majmaah,, Saudi Arabia. yasser.abdelrhman@mu.edu.sa and Mechanical Design and Production Engineering Department, Faculty of Engineering, Assiut University.
[3] Mechanical Design and Production Engineering Dept., Faculty of Engineering, Assiut University, Assit, Egypt. emadd123@aun.edu.eg
[4] Mechanical Design and Production Engineering Dept., Faculty of Engineering, Assiut University, Assiut, Egypt. shemygabr@aun.edu.eg

https://doi.org/10.21608/jesaun.2024.334433.1381

(FDM), which uses thermoplastic filaments to produce durable parts with high accuracy. The adaptability of FDM technology allows for its use in sectors such as automotive, aerospace, and healthcare, providing a cost-effective solution for rapid prototyping and functional part manufacturing [1–3].

Many different materials exist which can be used for FDM printing. Two widely used materials in FDM printing are Polypropylene (PP) and Polylactic Acid (PLA), although their application varies significantly in 3D printing. PLA is one of the most commonly used materials in FDM due to its ease of printing, low cost, and biodegradability. PLA's low thermal distortion makes it suitable for consumer-level 3D printers, as it prints at lower temperatures and does not require a heated bed, unlike other polymers. Its bio-based origin also makes it an attractive choice for environmentally conscious applications, particularly in packaging, medical devices, and prototyping [4]. In contrast, PP is less frequently used in FDM printing despite its widespread industrial use. PP is known for its excellent chemical resistance, high impact strength, and flexibility, making it ideal for use in automotive parts, chemical containers, and textiles. However, its application in 3D printing is limited due to several challenges. PP tends to warp during the printing process, making it difficult to print without specialized equipment, such as heated beds or enclosures, which are not always accessible on standard desktop 3D printers. Additionally, achieving good layer adhesion is more difficult with PP due to its lower surface energy. Despite these challenges, PP's outstanding mechanical properties and low density make it an appealing choice for certain high-performance applications, and ongoing research aims to improve its printability [5].

Both materials offer distinct advantages in 3D printing, with PLA dominating the consumer market due to its ease of use, while PP holds potential in more demanding industrial applications where flexibility and chemical resistance are key. In general, thermoplastics have limitations in strength, stiffness, and mechanical properties. By reinforcing these polymers with fillers, their mechanical properties can be further enhanced, making them suitable for a wider range of functional applications [6]. Composite filaments incorporate various reinforcement materials, such as particulate fillers, fibers, and nanocomposites, to boost mechanical, thermal, and sometimes electrical properties, as well as biocompatibility in printed parts [7–11]. Common reinforcement fibers include carbon and glass, which enhance the material's strength-to-weight ratio, thermal stability, and performance characteristics. Fiber-reinforced polymer composites (FRPCs) owe their improved properties to factors like fiber type, polymer matrix, interfacial bonding, void content, fiber volume fraction, and fiber orientation. Carbon fibers are particularly effective in composites due to their high tensile strength, lightweight, stiffness, heat tolerance, and chemical resistance. Adding carbon fibers to thermoplastics also helps stabilize their thermal properties and minimizes warping.

In fiber-reinforced composites, fibers can either be continuous or short, which significantly affects the composite's properties. Composites are thus classified as continuous fiber-reinforced (fiber length > 50 mm) or short fiber-reinforced (fiber length < 1 mm), each suited to different applications based on performance requirements [12]. Several studies have investigated the reinforcement of polypropylene (PP) and polylactic acid (PLA) with fibers, providing valuable insights into the mechanical improvements achievable through such modifications. For instance, Ning et al. [13] studied carbon fiber-reinforced PP composites, finding significant improvements in tensile strength and Young's modulus. However, they also observed reductions in properties like yield strength, ductility, and toughness. Similarly, Pollini et al. [14] found that adding 14 wt% of short carbon fibers (SCF) to recycled PP increased tensile strength (from 19.72 to 22.70 MPa) and Young's modulus (from 961.5 to 1352.33 MPa), though it decreased the material's elongation at break. Spork et al. [15] demonstrated that fiber orientation in 3D-printed PP composites not only enhanced mechanical properties but also improved thermal conductivity along the printing

direction. While higher SCF content further increased mechanical strength, it came at the cost of reduced ductility.

For PLA composites, Blok et al. [16] compared continuous and short carbon fiber reinforcement, noting that continuous fibers provided superior mechanical strength, despite some printing challenges. Thirugnanasamabandam et al. [17] found that carbon fiber-reinforced PLA laminates demonstrated mechanical performance similar to carbon-fiber-reinforced plastics (CFRP). Papen and Hague [18] observed enhanced fracture toughness in PLA composites containing milled carbon fibers. Additionally, Saleh et al. [6] showed that recycled carbon fiber (rCF) PLA composites increased tensile modulus by 58.30%, though there was a slight reduction in tensile strength.

Together, these studies illustrate that fiber reinforcement effectively enhances the mechanical properties of PP and PLA composites, though the specific effects vary based on fiber content, type, and orientation. Most of the previous studies have focused on optimizing strength in PLA and PP composites reinforced with carbon fibers. However, limited research has explored the effects of varying percentages of micro carbon fiber (MCF) in PLA and PP composites. This study addresses this gap by examining the production, process ability, thermal, hydrophilic, mechanical, and morphological properties of MCF-reinforced PLA and PP composites, with MCF content ranging from 1 to 24 wt%. The composite materials were fabricated using the FDM method. Additionally, we employed Gaussian Process modeling in machine learning to compare its predictions with experimental results, offering deeper insights into the mechanical behavior of these composites.

2. Methodology

2.1 Materials

This research utilized two types of thermoplastic matrices: polylactic acid (PLA) and polypropylene (PP). PLA granules were obtained from Lynx-Additive Manufacturing Ltd (Cairo, Egypt) [19]. And have a melting temperature range of 180°C to 215°C. PP granules were supplied by ElDawlia ICO (Assiut, Egypt) [20]. Both polymers were reinforced with micro carbon fiber (MCF) sourced from Easy Composites Ltd (London, UK) [21]. According to the supplier, these MCFs have an average fiber length of 100 μm and a diameter of approximately 7 μm. The fibers were produced by carbonizing polyacrylonitrile (PAN) precursors, achieving a carbon content greater than 98%. The properties of PLA, PP, and MCF, as specified by the suppliers, are summarized in Table 1 according to suppliers.

Table 1. Mechanical properties for PP/ PLA according to suppliers.

Materials / properties	Polypropylene (PP)	Polylactic acid (PLA)	Carbon fiber (CF)	Units
Density	900	1240	400	Kg/m^3
Melting point	165	175 ~ 210	3652 ~ 3697	^{O}C
Tensile strength	17	39	4150	MPa
Elongation at break	> 400	> 10	N/A	%

2.2 Filament extrusion process

The filament production setup comprises three main components: an extruder, a water bath, and a pulling mechanism, as shown in Figure 1 . A custom-built screw extruder, located at Assiut

University's facilities, was used to fabricate the filament. This extruder includes a nozzle with an internal diameter of 3 mm and is equipped with a DC motor for variable speed control. A specifically engineered puller mechanism functions as a filament receiver, designed to draw the filament at a consistent speed while maintaining steady tensile strength.

The cooling process was enhanced with a water bath, which proved more efficient than air-blowing methods. Extrusion was carried out at a temperature of 190°C for PP and 160 for PLA, with heaters positioned before the die and at the end of the compression zone maintained at the same temperature. For optimal material feed, the screw rotated at a speed between 12 and 15 rpm. Adjustments to the filament diameter were made by coordinating the speed of the puller mechanism with the extrusion output rate. The filament receiving point of the puller mechanism was positioned 1.3 m from the nozzle. All processing parameters for producing MCF/PLA and MCF/PP composite filaments were optimized to ensure a uniform circular profile with an average diameter of 1.75 mm, suitable for 3D printing, as detailed in Table 3. Pristine PLA and PP filaments were produced under comparable conditions as a control. Filament extrusion followed standard procedural guidelines as referenced in prior studies [22,23]. Figure 2 illustrates the whole process as a flowchart.

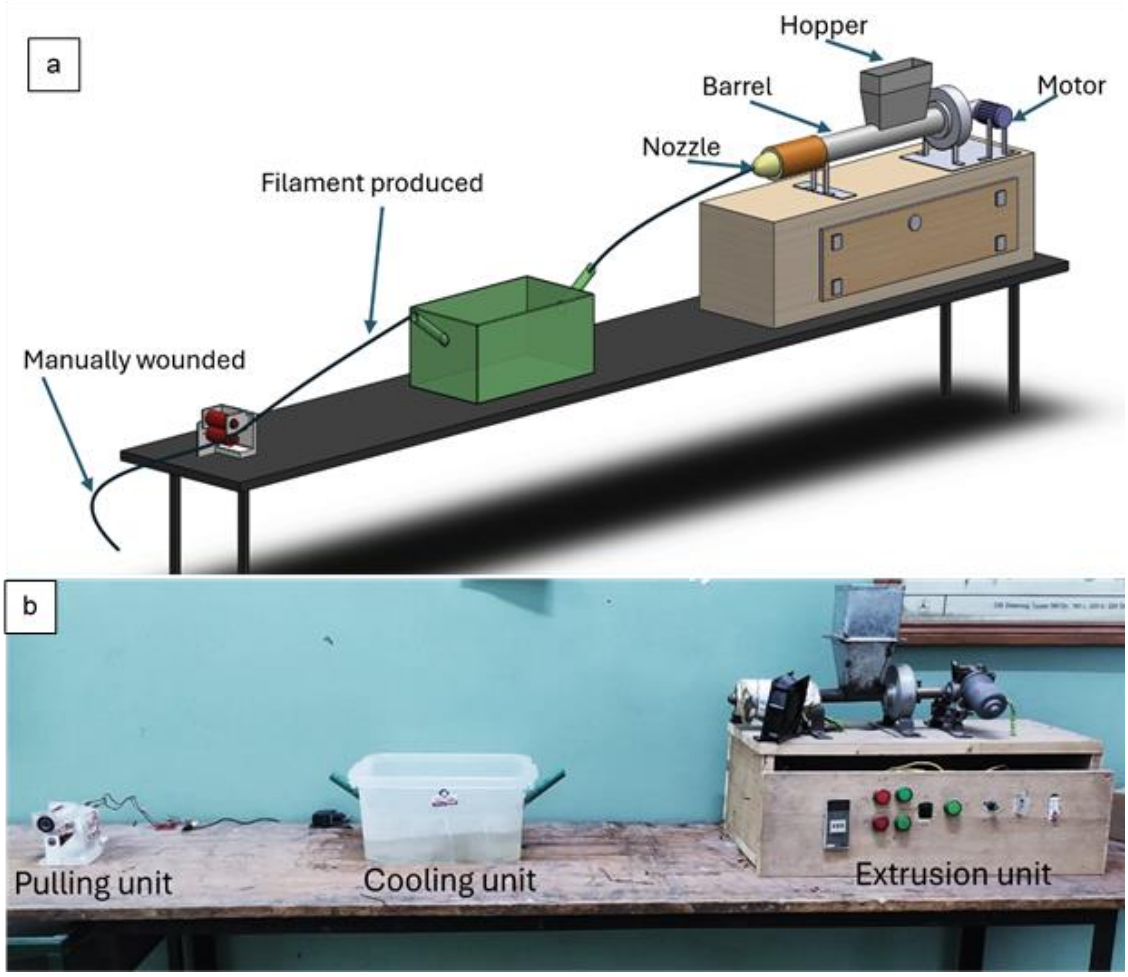

Figure **1**. Filament maker: (a) CAD model, and (b) actually model

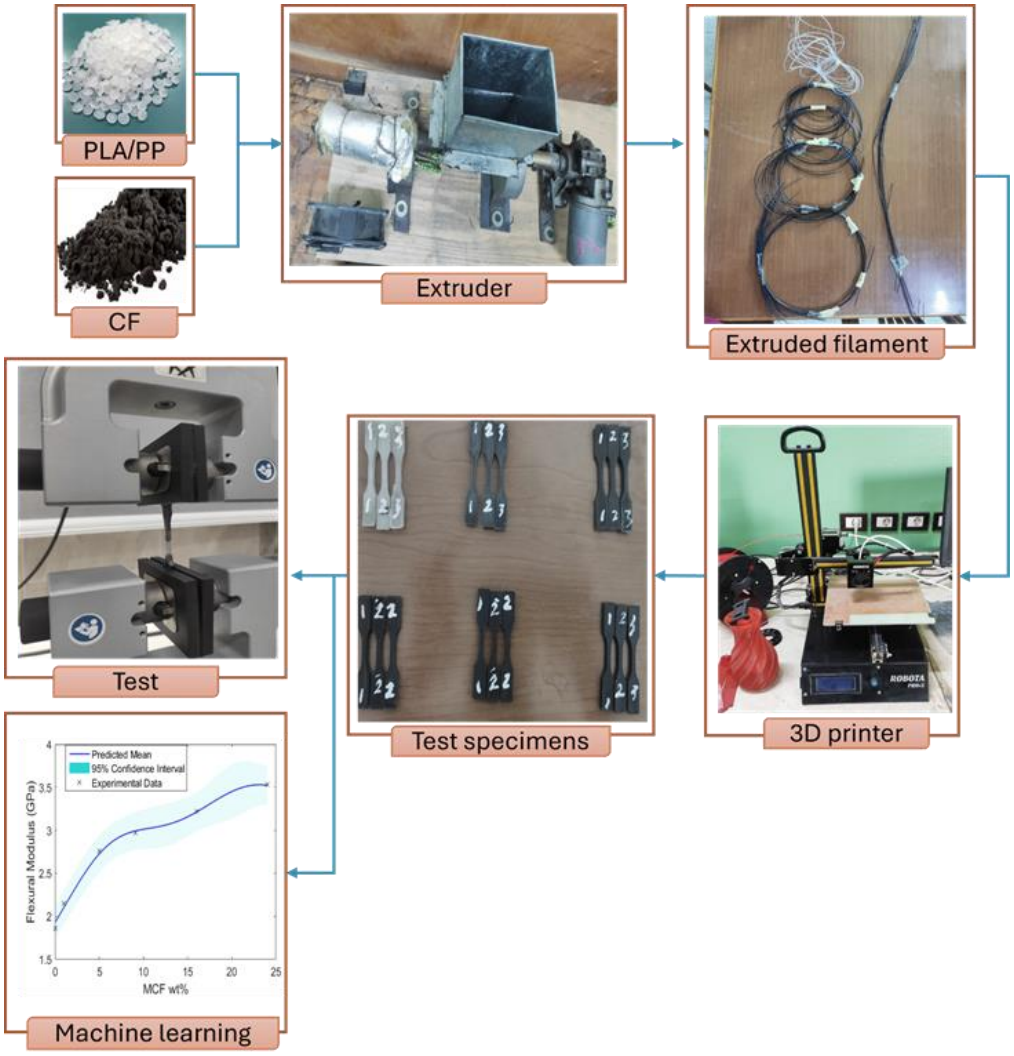

Figure **2**. Flowchart showing the process from filament fabrication to testing and GPR predictions.

2.3 3D printing process

All neat PP, PLA, and composite samples were fabricated using a commercial Robot Pro +2 3D printer (Egypt) equipped with a 0.4 mm nozzle. The samples were first designed in SolidWorks and then converted to G-code for compatibility with the printer. Cure software was used to fine-tune the printing parameters for both neat and composite materials, ensuring optimal print quality. To enhance bed adhesion and minimize warping, a raft was applied to the bottom of each sample, allowing for easy removal after printing. The specific printing parameters used in these tests are provided in Table 2.

Table 2. 3D printing parameters used.

Parameters	Value	Unit
Infill pattern (Grid)	45/135	degree
Layer thickness	0.2	mm
Bed temperature	65	^{O}C
Nozzle temperature	190/255 (PLA/PP)	^{O}C
Fill density	100	%
Motion speed	28/20 (PLA/PP)	mm/s

2.4. Testing process

Mechanical testing: Tensile and flexural tests were conducted on neat PLA, PP, and their carbon fiber-reinforced composites using a universal testing machine (Intron model 3366, US) equipped with a 10 kN load cell, The displacement measurement accuracy of the machine is specified as ±0.02 mm or 0.15% of the total measured displacement, depending on which value is greater. This ensures precise displacement readings across various testing conditions. These tests measured key mechanical properties, including tensile strength, modulus of elasticity, and elongation at break, flexural strength, and flexural modulus.

For tensile testing, the samples were prepared following ASTM D638 Type V [24] specifications, optimized for FDM-printed samples. Tests measured tensile strength and elongation at a displacement rate of 10 mm/min, with three samples tested per composition for consistency. Flexural tests adhered to the ASTM D790-10 [25] standard for three-point bending on rectangular specimens, maintaining the same displacement rate. Again, three samples per composition were tested to ensure reliable results.

Figure 3 displays the tensile, flexural, and water absorption test specimens, offering a clear visual of the sample geometries used. These tests provided essential insights into the mechanical performance of PLA and PP composites, with and without carbon fiber reinforcement, helping to understand the materials' behavior under different loading conditions.

Optical microscope examination: The PME OLYMPUS TOKYO optical microscope was used to examine the fractured surfaces of PLA and PP composite samples after mechanical testing, as well as the cross-sections of the filament samples. This analysis provided detailed insights into microstructural features, including voids, cracks formed post-fracture, and fiber distribution within the matrix. Optical imaging captured essential details on fiber alignment, dispersion, and bonding with the matrix, facilitating the evaluation of failure mechanisms and internal structure. Each sample surface was carefully prepared prior to imaging to ensure accurate assessment of fiber integration and fracture patterns.

Water absorption testing: The water absorption test followed ASTM D570 [26]. Specimens measuring 30 x 10 x 3 mm, both for PLA and MCF/PLA composites, were conditioned for 24 hours at room temperature. After conditioning, the samples were fully immersed in a water bath. Over a 30-day period, the specimens were removed every 72 hours, thoroughly dried with paper towels, and weighed using a digital balance with 0.1 mg precision to determine water uptake. The percentage increase in mass was calculated using Equation 1, ensuring accurate and consistent tracking of water absorption throughout the test.

$$\boldsymbol{w}(\%) = \frac{\boldsymbol{w_f - w_i}}{\boldsymbol{w_i}} \times \mathbf{100} \qquad (1)$$

Where w represents the percentage of water absorption, w_f is the mass absorbed after specific time t, and w_i represents the initial mass without any water gain.

The diffusion coefficient (Dx) for each material was calculated using Equation 2, which is derived from the slope of the first linear region on a graph plotting water weight gain against the square root of time. This method ensures an accurate representation of how each material absorbs water over time, as detailed in reference[27].

$$D_x = \pi\left(\frac{h}{4M_{sat}}\right)^2 \left(\frac{M_t}{\sqrt{t}}\right)^2 \quad (2)$$

Where (t) is the immersion duration, (h) is the specimen thickness, and (M_{sat}) is the saturated water content percentage. This equation represents the relationship between immersion time, thickness, and water content.

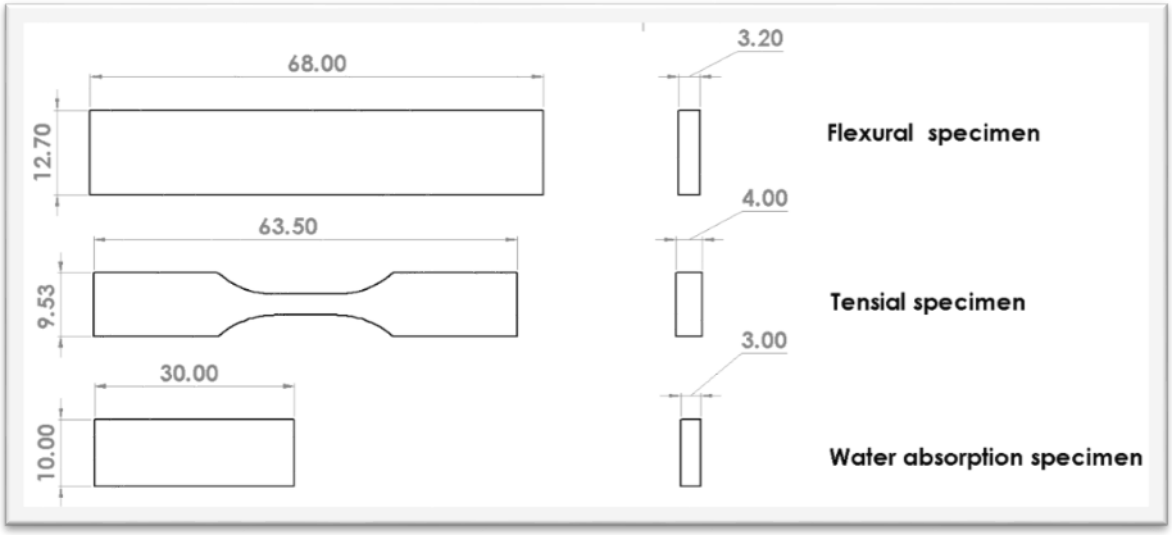

Figure 3. Geometry of tested specimens

Prediction of mechanical properties using Gaussian process regression: Gaussian Process Regression (GPR) is a versatile, probabilistic, non-parametric technique employed to predict relationships between inputs and outputs without requiring a predetermined function. It operates under the assumption that observed data follows a joint Gaussian distribution characterized by a mean and a covariance function, or kernel. This flexibility makes GPR particularly effective for accurately predicting patterns, such as mechanical properties.

The kernel function denoted as $k(x_1, x_2)$ encodes prior knowledge and influences the smoothness or periodicity of the model. A widely used kernel is the Radial Basis Function (RBF), defined by the equation:

$$k(x_1, x_2) = \sigma_f^2 \exp\left(-\frac{(x_i - x_j)}{2l^2}\right) \quad (3)$$

where σ_f^2 is the signal variance, l is the length scale, and x_i and x_j are input points [28].

In this study, MATLAB was utilized to implement GPR for predicting the tensile strength and modulus of PLA, PP, and their composites, leveraging experimental data. MATLAB's GPR functions enabled efficient model training, visualization, and prediction with confidence intervals, which are crucial for assessing uncertainties in predictions. The model was trained using experimental data related to material compositions and measured mechanical properties, such as tensile strength. Once trained, the model could predict properties for new compositions, providing expected values alongside confidence intervals to evaluate prediction reliability.

This capability is particularly beneficial in materials science, where understanding uncertainties is essential for optimizing material selection and processing parameters, ultimately reducing the need for extensive experimental testing.

3. Results and discussion

3.1.Tensile properties comparison

Figure 4 illustrates the tensile stress-strain behavior of polypropylene (PP) and polylactic acid (PLA) composites with varying micro carbon fiber (MCF) content, highlighting the distinct impacts of carbon fiber reinforcement on tensile strength and ductility. Both materials show enhanced tensile properties with carbon fiber additions at lower concentrations, although their optimal reinforcement thresholds differ; PP composites retain improved tensile strength and ductility up to approximately 9.09% MCF, while PLA composites achieve optimal performance at around 5% MCF. Beyond these limits, both materials exhibit more brittle behavior and a reduction in tensile strength, with PLA being more adversely affected by high carbon fiber content than PP. The mechanical properties derived from Figure 4 are further detailed in Figures 5, 6, and 7, which present the ultimate tensile strength, modulus of elasticity, and tensile strain at break for PP and PLA composites with varying carbon fiber (CF) content. Figure 5 presents a bar chart comparing the tensile strength of PP and PLA composites at various CF weight percentages. For PLA, tensile strength increases with small additions of CF, peaking at 1% CF. Beyond this point, it gradually declines as CF content increases. Similarly, PP composites show an improvement in tensile strength at lower CF levels. However, tensile strength decreases when the CF content exceeds 5%. At 24% CF, both materials exhibit a noticeable reduction in tensile strength. Across all CF levels, PLA consistently demonstrates higher tensile strength than PP. These findings suggest that low CF concentrations improve tensile strength. However, higher CF levels may lead to diminishing returns or reductions due to factors such as fiber dispersion or compatibility issues within the polymer matrix [29,30]. Figure 6 compares the strain at break for PP and PLA composites across different CF concentrations, highlighting a significant difference in strain behavior. PP exhibits high initial ductility, with a strain at break of approximately 245% in the absence of CF. However, as CF content increases, the strain at break decreases sharply, dropping below 50% at higher CF levels [31]. In contrast, PLA shows consistently low strain at break across all CF concentrations. This indicates that the addition of CF has a much greater impact on reducing the flexibility of PP than it does for PLA. Figure 7 displays a scatter graph illustrating the modulus of elasticity for PP and PLA composites as a function of CF content. The data show that stiffness increases for both materials with higher CF concentrations. However, PLA consistently demonstrates a higher modulus of elasticity than PP at all CF levels. This characteristic makes PLA more suitable for applications requiring greater rigidity. On the other hand, PP's ability to maintain adaptability and accommodate higher CF levels without losing ductility and strength makes it a preferable option for applications that demand a balance of strength and flexibility. The constant stress region observed in PLA composites curves can be attributed to the deboning process between short carbon fibers and the polymer matrix, where the load is temporarily redistributed, delaying further stress buildup. This phenomenon, typical in fiber-reinforced composites, reflects the inelastic response of the material due to localized stress concentrations or imperfections in fiber distribution. In summary, both materials benefit from carbon fiber reinforcement, but PP can tolerate higher CF content

before significant losses in ductility and strength, while PLA's stiffness may be more advantageous in applications prioritizing rigidity.

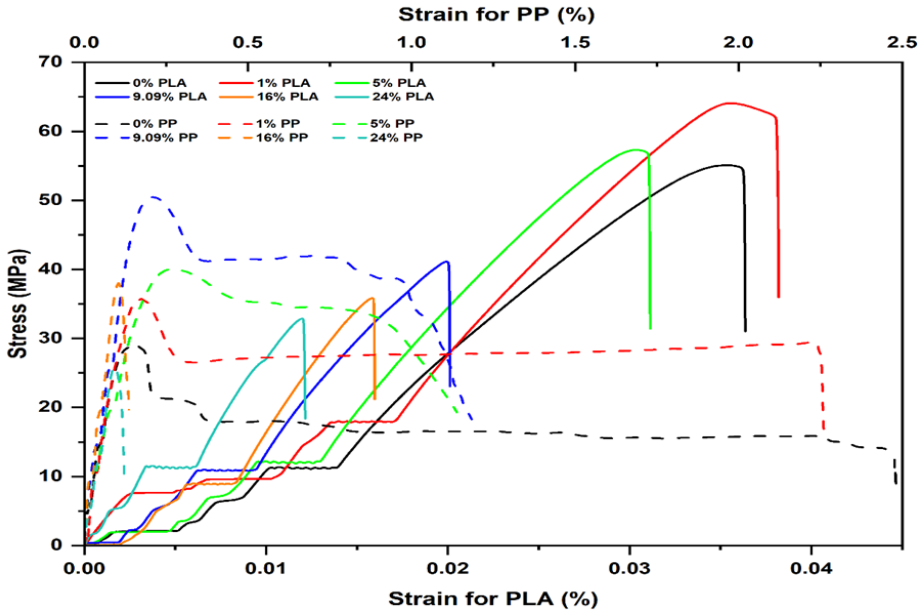

Figure 4. Tensile behavior of PP and PLA composites with varying carbon fiber ratios, showing tensile strength changes with strain

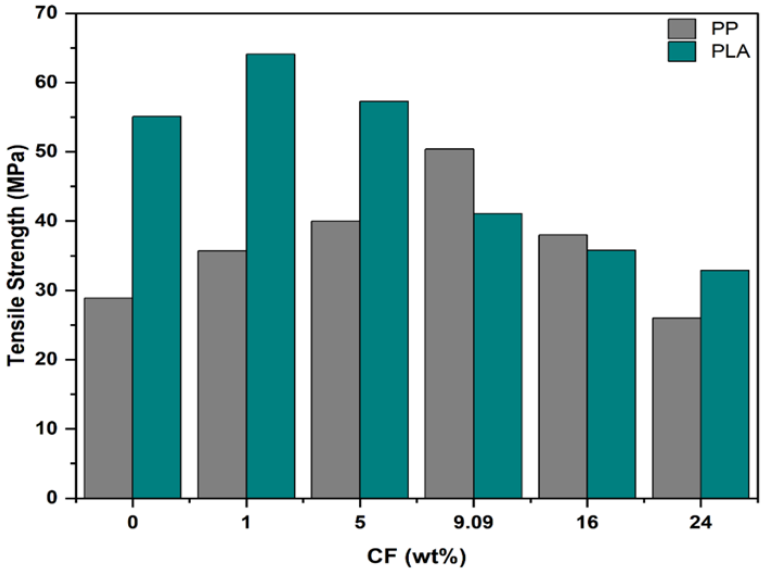

Figure 5. A bar chart comparing the tensile strength of PP and PLA composites across different carbon fiber concentrations.

3.2 Flexural properties comparison

Figure 8 and Figure 9 compare the flexural properties of polypropylene (PP) and polylactic acid (PLA) composites at various carbon fiber (CF) concentrations. In Figure 8, the histogram illustrates that flexural strength for both PP and PLA initially increases with added CF, peaking at specific CF concentrations before declining at higher fiber loads, likely due to issues like poor fiber dispersion or weakened material cohesion. Across all CF levels, PLA consistently demonstrates higher flexural strength than PP, indicating greater bending resistance. Figure 9, which shows the flexural modulus as a measure of stiffness, reveals that both PP and PLA composites experience an increase in

rigidity as CF content rises, with PLA maintaining a higher flexural modulus than PP throughout. This consistent trend suggests that PLA composites are stiffer than PP composites at each CF concentration, making them more suitable for applications where high rigidity and strength in bending are essential. Together, these figures underscore that while CF reinforcement improves both flexural strength and modulus in PP and PLA, PLA generally performs better in terms of bending resistance and stiffness, especially in applications requiring enhanced structural stability.

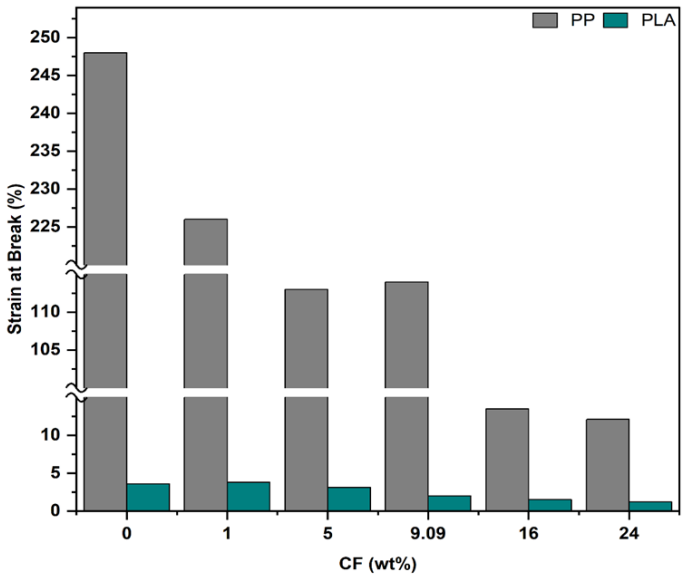

Figure 6. A bar chart comparing the strain at break of PP and PLA composites across different carbon fiber concentrations.

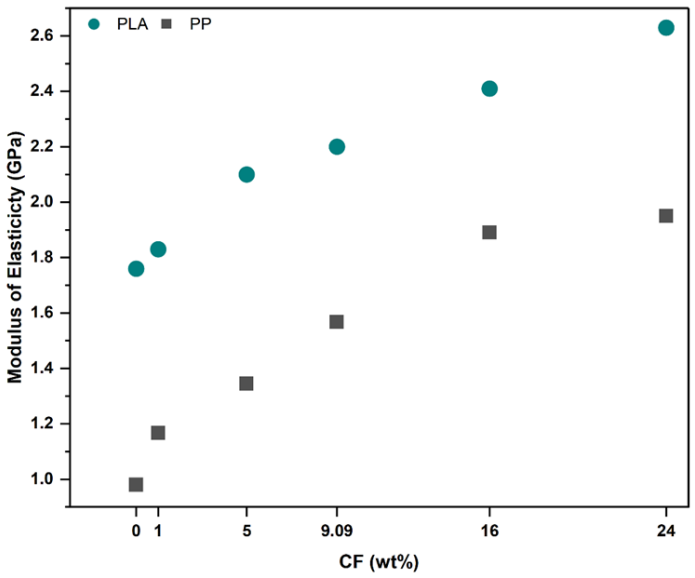

Figure 7. Comparison graph of the modulus of elasticity for PP and PLA composites at different carbon fiber concentrations.

3.3 Microscopy examination

This section examines the morphology of both the filaments and the fracture surfaces of carbon fiber-reinforced PLA and PP composites using optical microscopy to understand failure mechanisms. The analysis focuses on the shape and distribution of fibers within the filament cross-sections, as well as the fracture characteristics observed in samples after mechanical testing. By comparing these images, we aim to assess how carbon fiber dispersion and interaction affect the structural integrity, fracture behavior, and overall performance of the composites. This analysis highlights the role of fiber distribution in contributing to mechanical properties and influencing material failure modes.

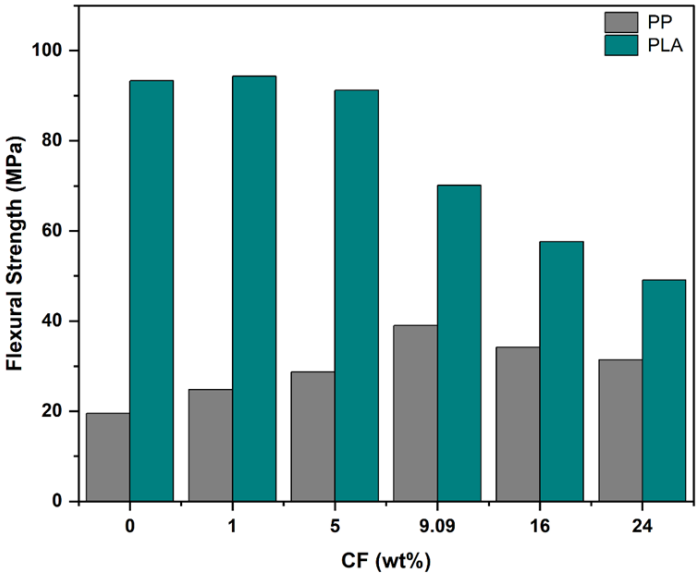

Figure 8. A bar chart comparing the flexural strength of PP and PLA composites across different carbon fiber concentrations.

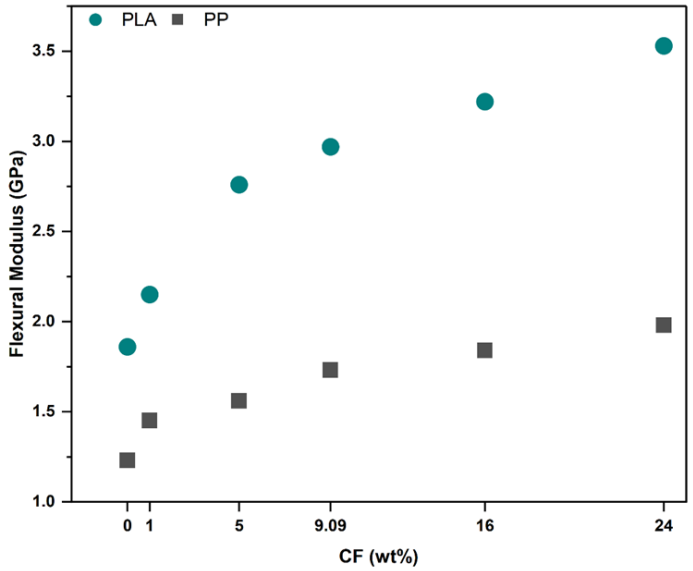

Figure 9. Comparison graph of the flexural modulus for PP and PLA composites at different carbon fiber concentrations.

The optical microscope images provide cross-sectional views of filaments composed of PLA with 16 wt% carbon fiber (Figure 10, a) and PP with 16 wt% carbon fibers (Figure 10, b). In both images, the carbon fibers appear as nearly circular dark regions, representing the fiber ends exposed by cross-sectioning for imaging. This alignment indicates that most fibers are oriented parallel to the filament axis, contributing to enhanced tensile strength along this direction. In Figure 10, b (PP with 16 wt% CF), some voids are visible, likely formed during the manufacturing process due to trapped air bubbles. These voids may act as stress concentrators, potentially impacting mechanical performance by reducing the material's overall strength and creating points of weakness.
Both images show a generally uniform distribution of fibers within the polymer matrix, which is crucial for achieving favorable mechanical properties. A well-dispersed and homogeneously distributed fiber network enhances the composite's strength and stiffness by facilitating better load transfer from the polymer matrix to the reinforcing fibers. Furthermore, the observed fiber alignment suggests controlled orientation during filament fabrication, which may be beneficial for applications where directional mechanical properties are essential.

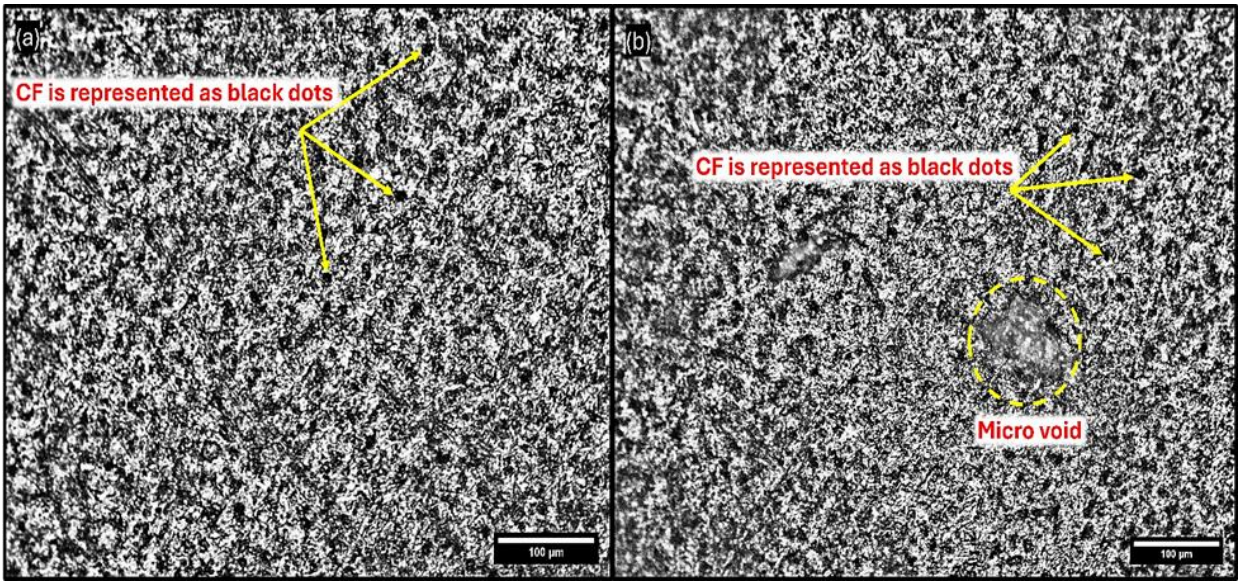

Figure 10. OM images of filament cross-sections for: (a) PLA with 16 wt% CF, and (b) PP with 16 wt% CF.

The optical micrographs in Figure 11 show fracture surface morphologies of polypropylene (PP) and polylactic acid (PLA) composites, each reinforced with 24 wt% carbon fibers, after tensile testing. The fracture surface analysis of polypropylene (PP) and polylactic acid (PLA) composites highlights distinct differences in their tensile fracture behaviors due to the inherent mechanical properties of the matrices. PP composites exhibit ductile fracture characteristics, with visible micro-voids, fiber pull-out, and significant matrix elongation under load, which allow energy absorption through plastic deformation as shown in Figure 11,(a-c) [32]. This indicates that the PP matrix can stretch, redistributing stress around the fibers and delaying catastrophic failure. In contrast, PLA composites show brittle fracture features, with sharp, clean edges and limited matrix deformation, suggesting a rapid and brittle failure mechanism due to PLA's higher stiffness and lower ductility as illustrated in Figure 11,(d-f) [33]. While fiber pull-out in PP composites suggest moderate fiber-matrix bonding conducive to toughness, the PLA composites show minimal fiber pull-out, leading to a stronger but more brittle bond that lacks significant energy-absorbing capability. Additionally, fiber agglomeration in PLA composites indicates uneven stress distribution, contributing to abrupt

fractures and reflecting the brittle nature of PLA. The high fiber content in both composites reduces the available matrix volume, further restricting deformation in PLA and resulting in a sudden, brittle fracture, whereas in PP, it allows continued matrix elongation and void formation, enhancing toughness. Overall, PP composites are better suited for applications requiring ductility and energy absorption, while PLA composites are preferable for applications demanding stiffness, though they are more susceptible to brittle failure under tensile stress.

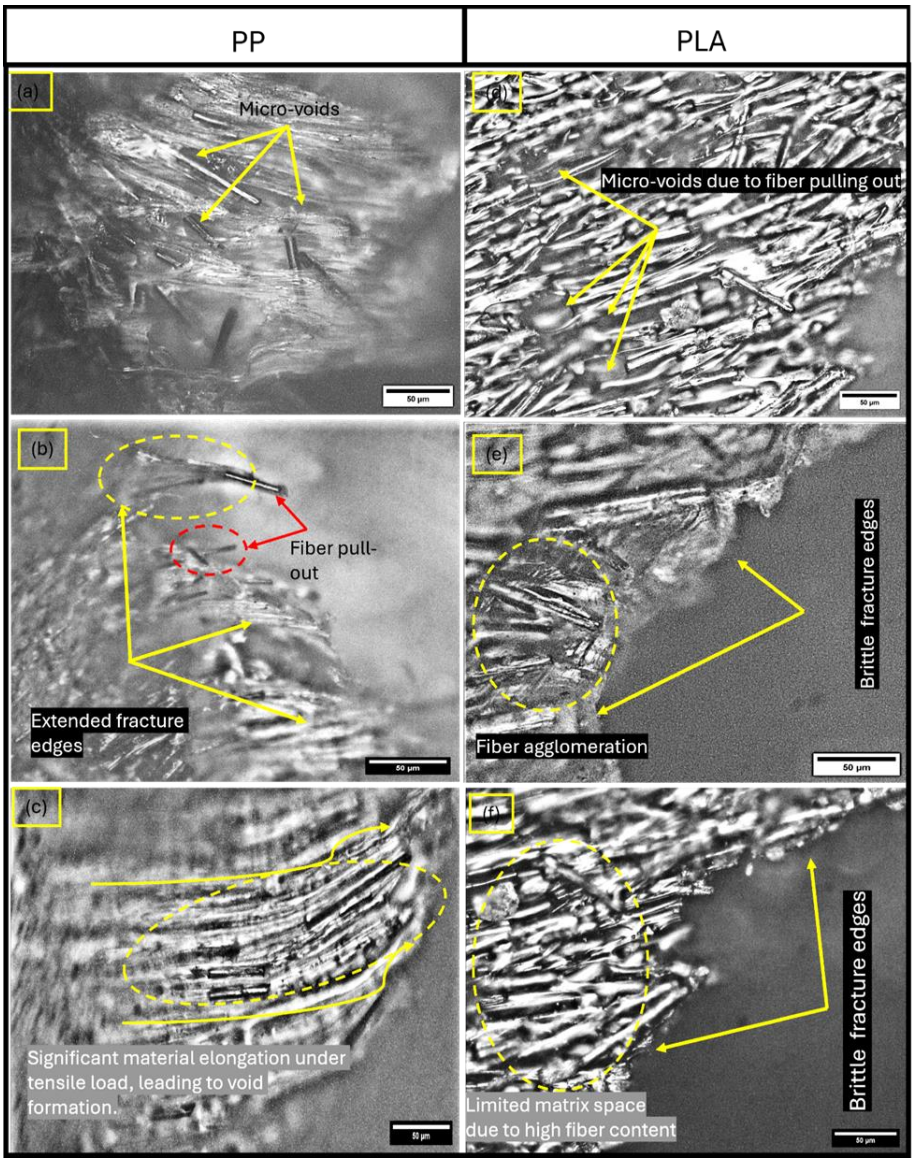

Figure 11. Optical micrographs of fracture surfaces post-tensile testing: (a-c) PP and (d-f) PLA with 24 wt% carbon fibers.

3.4.Water absorption behavior

By observation Figure 12, at lower carbon fiber concentrations (9.09 wt% and below), PLA consistently shows higher water absorption compared to PP. This difference is attributed to PLA's more hydrophilic nature, allowing it to absorb more water early in the process. The water absorption rate in PLA stabilizes after the first few days, with a maximum of around 7-9% at 9.09 wt%. However, when the carbon fiber concentration increases to 16 wt% and 24 wt%, the absorption rate in PLA rises more slowly, reaching a peak of approximately 13% for the highest

carbon content. The lower overall absorption rate at higher carbon content suggests that the microstructure of PLA changes in a way that reduces water retention despite the increased porosity caused by carbon fibers. In contrast, PP absorbs significantly less water than PLA at fiber contents below 9.09 wt%, showcasing its hydrophobic properties. As the carbon fiber content reaches 16 wt% and 24 wt%, PP begins to absorb more water than PLA. The water absorption at 24 wt% in PP reaches approximately 14%, higher than PLA at the same concentration. The increase in water absorption in PP is likely due to the formation of micro-voids and greater porosity at higher carbon contents, trapping more water molecules within the composite.

Comparing both materials, at lower fiber concentrations, PLA shows more water absorption than PP due to its intrinsic material properties. However, at higher fiber concentrations, the trend reverses, with PP absorbing more water than PLA. This shift is primarily due to the increasing porosity of PP at higher carbon fiber concentrations, making it more susceptible to water retention. When examining the diffusion coefficient, as shown in Figure 13, we observe that it increases with carbon fiber content for both materials. However, PP exhibits a consistently higher diffusion coefficient across all carbon fiber concentrations compared to PLA. This suggests that while the diffusion behavior is similar in both materials, PP absorbs and diffuses water more rapidly, likely due to its higher porosity and the formation of voids around the fibers

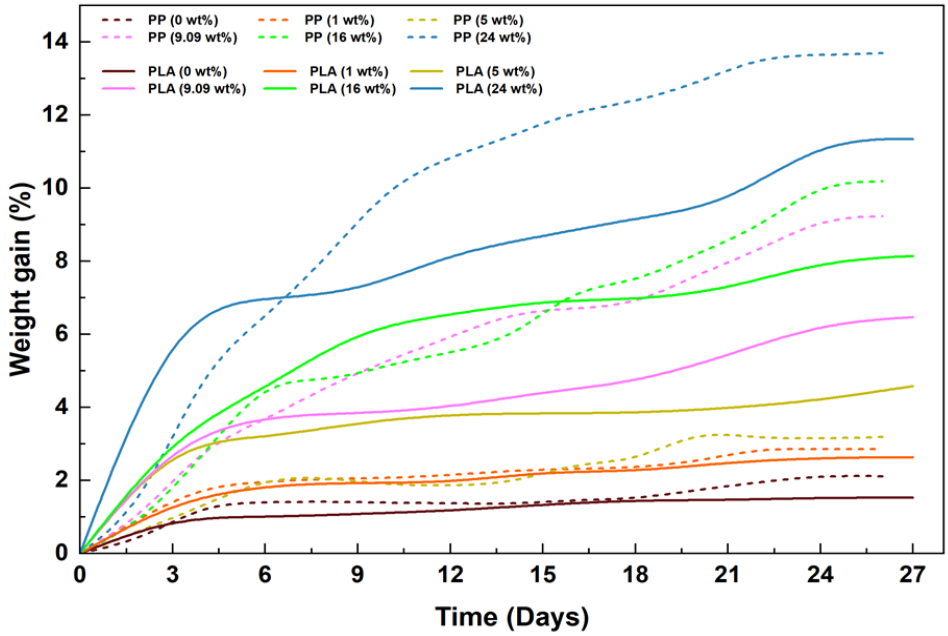

Figure 12. Water absorption behavior for PP and PLA composites at different carbon fiber concentrations.

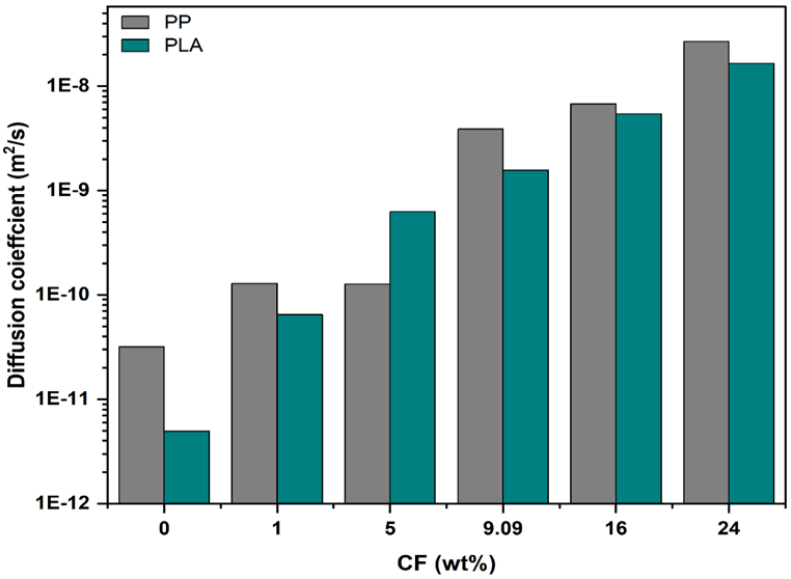

Figure 13. A bar chart comparing the diffusion coefficient of PP and PLA composites across different carbon fiber concentrations

3.5.Tensile properties predictions

Using the GPR model through MATLAB, a comparison was made between the tensile test results of PLA and PP. The model allowed us to predict intermediate values (between the experimentally measured values) for carbon fiber concentrations ranging from 0 to 24 wt%. This prediction capability extends to tensile strength, modulus of elasticity, or strain at break for any given carbon concentration within this range, despite only having measured six data points experimentally, as discussed earlier.

In Figure 14, (a) , which presents the tensile strength predictions for both PP and PLA, it becomes clear that the highest predicted tensile strength for PLA could have occurred at approximately 2.5 wt% carbon concentration, with a value approaching 70 MPa. This is interesting, as it suggests a peak in tensile strength at a concentration that was not directly measured experimentally. On the other hand, the GPR prediction for PP aligns well with the experimental data, showing that the highest tensile strength is expected around the 9.09 wt% concentration.

In Figure 14, (b), which displays the predictions for the modulus of elasticity for both PLA and PP, the consistency between the GPR predictions and the experimental values is clear. The general trend shows that as the carbon fiber content increases, the modulus of elasticity rises in a nearly linear fashion for both materials. This consistency demonstrates the reliability of the GPR model in capturing the mechanical behavior of these composites.

Similarly, Figure 14, (c) illustrates the predicted strain at break, which also aligns well with the experimental values and logical expectations. For PP, the highest strain at break is observed in the carbon-free samples, which is reasonable given PP's high flexibility compared to PLA. As carbon is added, the strain decreases, as carbon fibers tend to increase stiffness and brittleness. On the other hand, PLA samples show a near-constant strain at break, slightly above zero, highlighting the significant difference in mechanical behavior between PLA and PP when subjected to loads. In summary, this predictive model is highly valuable for identifying and discovering the mechanical properties of carbon fiber-reinforced composites across all fiber concentrations without the need for extensive experimental testing. This approach saves time and resources by providing reliable predictions for untested concentrations.

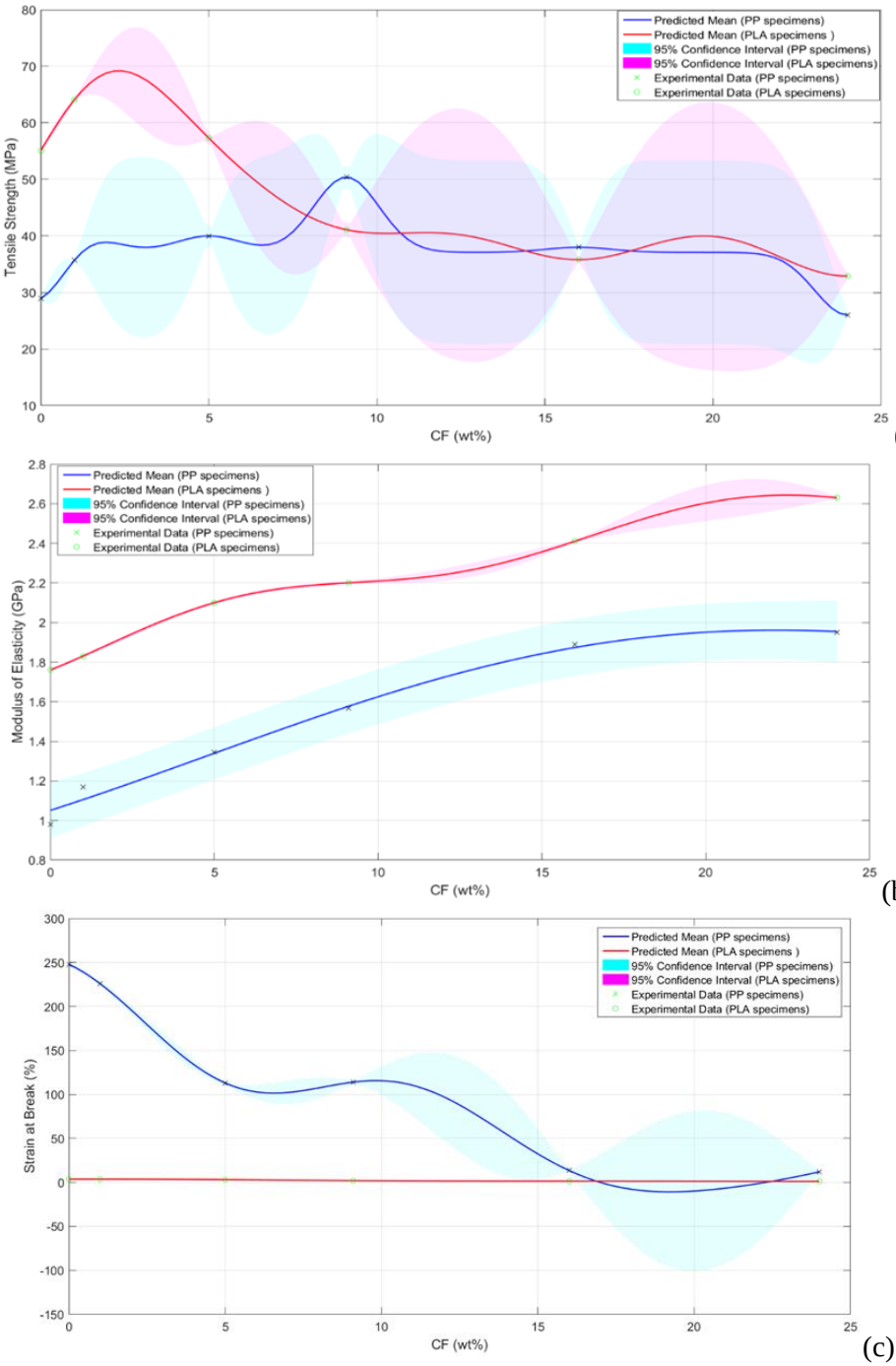

Figure 14. Comparison of predicted tensile strength (a), modulus of elasticity (b), and strain at break (c) for PP and PLA composites across varying carbon fiber content.

4. Conclusions

This study demonstrates the effectiveness of carbon fiber reinforcement in enhancing the mechanical properties of polypropylene (PP) and polylactic acid (PLA) composites for additive manufacturing applications. Both materials responded differently to carbon fiber addition, highlighting unique behaviors based on fiber concentration. The key findings are as follows:

- While PLA has an inherently high tensile strength, its mechanical performance showed diminishing returns as carbon fiber content increased, especially beyond 5 wt%. Small amounts of carbon fiber improved PLA's strength, but higher concentrations led to reduced tensile and flexural properties, likely due to poor matrix-fiber interaction at high loadings.
- PP showed significant improvements in tensile strength and flexural modulus with increasing carbon fiber content, with optimal performance observed at 9.09 wt%. At this concentration, PP reached peak tensile and flexural properties, after which further fiber additions led to performance decline.
- Optical microscopy of fracture surfaces showed that PLA with a lot of carbon fiber had brittle fracture patterns, while PP had more ductile fracture patterns, which are due to its toughness and ability to bend plastically.
- PLA displayed higher water absorption at lower carbon fiber concentrations, reflecting its more hydrophilic nature compared to PP. At higher carbon fiber content, however, PP exhibited increased water retention due to enhanced porosity.
- The Gaussian Process Regression (GPR) model correctly predicted mechanical properties across untested carbon fiber concentrations. This made it possible to find the best levels of reinforcement without having to do a lot of tests. This model streamlines material selection and facilitates targeted property enhancement for specific engineering applications.

In conclusion, carbon fiber reinforcement effectively tailors the mechanical properties of both PP and PLA. PP benefits more from moderate carbon fiber additions, which optimize its toughness and strength, whereas PLA achieves better performance with minimal reinforcement, preserving its inherent strength. These insights provide valuable guidance for the selection and optimization of reinforced composites in additive manufacturing applications.

References

[1] Shulga, E., Karamov, R., and Sergeichev, I. S., 2020, “Fused Filament Fabricated Polypropylene Composite Reinforced by Aligned Glass Fibers,” Materials (Basel). (13), pp. 3442–3451. [Online]. Available: https://www.mdpi.com/1996-1944/13/16/3442.

[2] Liu, J., Gaynor, A. T., Chen, S., Kang, Z., Suresh, K., Takezawa, A., Li, L., Kato, J., Tang, J., Wang, C. C. L., Cheng, L., Liang, X., and To, A. C., 2018, “Current and Future Trends in Topology Optimization for Additive Manufacturing,” Struct. Multidiscip. Optim. 57(6), pp. 2457–2483. https://doi.org/10.1007/s00158-018-1994-3.

[3] Heshmat, M., and Abdelrahman, Y., 2021, “Improving Surface Roughness of Polylactic Acid (PLA) Products Manufactured by 3D Printing Using a Novel Slurry Impact Technique,” Rapid Prototyp. J., 27(10), pp. 1791–1800. https://doi.org/10.1108/RPJ-09-2020-0227.

[4] Heshmat, M., Maher, I., and Abdelrahman, Y., 2023, “Surface Roughness Prediction of Polylactic Acid (PLA) Products Manufactured by 3D Printing and Post Processed Using a Slurry Impact Technique: ANFIS-Based Modeling,” Prog. Addit. Manuf., 8(2), pp. 87–98. https://doi.org/10.1007/s40964-022-00314-6.

[5] Romero, L. M., Esquivel, S. E., Montaño, M. C., Medina-Muñoz, C., Sánchez-Sanhueza, G. A., Palacio, D. A., Jaramillo, A. F., and Meléndrez, M. F., 2024, "Polypropylene with Clay–Filled for Fused Filament Fabrication: Comparative Study of the Mechanical Performance of Injected and 3d Printed Composite," Int. J. Adv. Manuf. Technol., 130(9), pp. 4251–4262. https://doi.org/10.1007/s00170-023-12889-7.

[6] Saleh, M., Anwar, S., AlFaify, A. Y., Al-Ahmari, A. M., and Abd Elgawad, A. E. E., 2024, "Development of PLA/Recycled-Desized Carbon Fiber Composites for 3D Printing: Thermal, Mechanical, and Morphological Analyses," J. Mater. Res. Technol., 29, pp. 2768–2780. https://doi.org/https://doi.org/10.1016/j.jmrt.2024.01.267.

[7] Li, J., Durandet, Y., Huang, X., Sun, G., and Ruan, D., 2022, "Additively Manufactured Fiber-Reinforced Composites: A Review of Mechanical Behavior and Opportunities," J. Mater. Sci. Technol., 119, pp. 219–244. https://doi.org/https://doi.org/10.1016/j.jmst.2021.11.063.

[8] Dickson, A. N., Barry, J. N., McDonnell, K. A., and Dowling, D. P., 2017, "Fabrication of Continuous Carbon, Glass and Kevlar Fibre Reinforced Polymer Composites Using Additive Manufacturing," Addit. Manuf., 16, pp. 146–152. https://doi.org/https://doi.org/10.1016/j.addma.2017.06.004.

[9] Durga Prasada Rao, V., Rajiv, P., and Navya Geethika, V., 2019, "Effect of Fused Deposition Modelling (FDM) Process Parameters on Tensile Strength of Carbon Fibre PLA," Mater. Today, Proc., 18, pp. 2012–2018. https://doi.org/https://doi.org/10.1016/j.matpr.2019.06.009.

[10] Ismail, K. I., Yap, T. C., and Ahmed, R., 2022, "3D-Printed Fiber-Reinforced Polymer Composites by Fused Deposition Modelling (FDM): Fiber Length and Fiber Implementation Techniques," Polymers (Basel). 14(21). https://doi.org/10.3390/polym14214659.

[11] Dickson, A. N., Abourayana, H. M., and Dowling, D. P., 2020, "3D Printing of Fibre-Reinforced Thermoplastic Composites Using Fused Filament Fabrication—A Review," Polymers (Basel). 12(10). https://doi.org/10.3390/polym12102188.

[12] Prüß, H., and Vietor, T., 2015, "Design for Fiber-Reinforced Additive Manufacturing," J. Mech. Des., 137(11), p. 111409. https://doi.org/10.1115/1.4030993.

[13] Ning, F., Cong, W., Qiu, J., Wei, J., and Wang, S., 2015, "Additive Manufacturing of Carbon Fiber Reinforced Thermoplastic Composites Using Fused Deposition Modeling," Compos. Part B Eng., 80, pp. 369–378. https://doi.org/10.1016/j.compositesb.2015.06.013.

[14] Pollini, M., Mutua, J. M., Mbuya, T. O., and Ernest, K., 2021, "Recipe Development and Mechanical Characterization of Carbon Fibre Reinforced Recycled Polypropylene 3D Printing Filament," Open J. Compos. Mater. 11(03), pp. 47–61. https://doi.org/10.4236/ojcm.2021.113005.

[15] Spork, M., Savandaiah, C., Arbeiter, F., Traxler, G., Cardon, L., Holzer, C., and Sapkota, J., 2018, "Anisotropic Properties of Oriented Short Carbon Fibre Filled Polypropylene Parts Fabricated by Extrusion-Based Additive Manufacturing," Compos. Part an Appl. Sci. Manuf., 113, pp. 95–104. https://doi.org/https://doi.org/10.1016/j.compositesa.2018.06.018.

[16] Blok, L. G., Longana, M. L., Yu, H., and Woods, B. K. S., 2018, "An Investigation into 3D Printing of Fibre Reinforced Thermoplastic Composites," Addit. Manuf., 22, pp. 176–186. https://doi.org/https://doi.org/10.1016/j.addma.2018.04.039.

[17] Thirugnanasamabandam, A., Subramaniyan, M., Prabhu, B., and Ramachandran, K., 2024, "Development and Comprehensive Investigation on PLA / Carbon Fiber Reinforced PLA Based Structurally Alternate Layered Polymer Composites," J. Ind. Eng. Chem., (xxxx). https://doi.org/10.1016/j.jiec.2024.02.012.

[18] Papen, E. A., and Hague, A., 2019, "Fracture Toughness of Additively Manufactured Carbon Fiber Reinforced Composites," Addit. Manuf., 26, pp. 41–52. https://doi.org/https://doi.org/10.1016/j.addma.2018.12.010.

[19] Plastic, T., "LynX Additive Manufacturing." [Online]. Available: https://www.lynx-am.com/.

[20] "Eldawlia ICO." [Online]. Available: https://www.eldawlia-ico.com/#home.

[21] Easycomposites, 2011, Carbiso Milled Carbon Fibre. [Online]. Available: http://www.elgcf.com/products/carbiso-milled-fibre.

[22] Taoufik Hachimia, Nassima Naboulsia, Fatima Majida, Rajae Rhanimb, I., and Mrania, H. R., 2021, "Design and Manufacturing of a 3D Printer Filaments Extruder," IGF26 - 26th Int. Conf. Fract. Struct. Integr. 33. [Online]. Available: e behavior can be changed by adding other po.

[23] Hasib, A. G., Niauzorau, S., Xu, W., Niverty, S., Kublik, N., Williams, J., Chawla, N., Song, K., and Azeredo, B., 2021, "Rheology Scaling of Spherical Metal Powders Dispersed in Thermoplastics and Its Correlation to the Extrudability of Filaments for 3D Printing," Addit. Manuf., 41, p. 101967. https://doi.org/https://doi.org/10.1016/j.addma.2021.101967.

[24] 2014, "ASTM D638-14. Standard Test Method for Tensile Properties of Plastics. West Conshohocken, PA, USA: ASTM International," ASTM D638-14. [Online]. Available: https://www.astm.org/d0638-14.html.

[25] 2016, "ASTM D790-10 Standard Test Methods for Flexural Properties of Unreinforced and Reinforced Plastics and Electrical Insulating Materials," ASTM D790-10. [Online]. Available: https://www.astm.org/d0790-10.html.

[26] 2022, "ASTM D570- 98 Standard Test Method for Water Absorption of Plastics," ASTM, ASTM D570- 98, West Conshohocken, PA, USA. [Online]. Available: https://www.astm.org/standards/d570.

[27] Banjo, A. D., Agrawal, V., Auad, M. L., and Celestine, A.-D. N., 2022, "Moisture-Induced Changes in the Mechanical Behavior of 3D Printed Polymers," Compos. Part C Open Access, 7, p. 100243. https://doi.org/https://doi.org/10.1016/j.jcomc.2022.100243.

[28] Saunders, R., Rawlings, A., Birnbaum, A., Iliopoulos, A., Michopoulos, J., Lagoudas, D., and Elwany, A., 2022, "Additive Manufacturing Melt Pool Prediction and Classification via Multifidelity Gaussian Process Surrogates," Integr. Mater. Manuf. Innov., 11(4), pp. 497–515. https://doi.org/10.1007/s40192-022-00276-1.

[29] Arun Kumar DT, Kaushik V Prasad, and P S Raghavendra Rao, 2015, "Study of Mechanical Properties of Carbon Fiber Reinforced Polypropylene," Int. J. Eng. Res., V4 (10), pp. 406–408. https://doi.org/10.17577/ijertv4is100500.

[30] Alkabbanie, R., Aktas, B., Demircan, G., and Yalcin, S., 2024, "Short Carbon Fiber-Reinforced PLA Composites: Influence of 3D-Printing Parameters on the Mechanical and Structural Properties," Iran. Polym. J., 33(8), pp. 1065–1074. https://doi.org/10.1007/s13726-024-01315-8.

[31] Mohd Yasin, S. B., Terry, J. S., and Taylor, A. C., 2023, "Fracture and Mechanical Properties of an Impact Toughened Polypropylene Composite: Modification for Automotive Dashboard-Airbag Application," RSC Adv., 13(39), pp. 27461–27475. https://doi.org/10.1039/D3RA04151D.

[32] Sodeifian, G., Ghaseminejad, S., and Yousefi, A., 2018, "Mechanical and Morphological Properties of Polypropylene/Short Glass Fiber /POE-g-MA Composite Manufactured by Fused Deposition Modeling (FDM) and CM Methods," The 10th International Chemical Engineering Congress & Exhibition (IChEC 2018).

[33] Mastalygina, E. E., and Aleksanyan, K. V, 2024, "Recent Approaches to the Plasticization of Poly (Lactic Acid) (PLA) (A Review)," Polymers (Basel). 16(1). https://doi.org/10.3390/polym16010087.

عنوان البحث: الآثار المقارنة لتدعيم كلا من البوليروبيلين وحمض البولي لاكتيك بألياف الكربون لأغراض الطباعة ثلاثية الأبعاد

الملخص :

تقدم هذه الدراسة تقييمًا مقارنًا لتأثير تعزيز ألياف الكربون على مصفوفتين من البولي بروبيلين (PP) وحمض البولي لاكتيك(PLA) ، مع التركيز على تطبيقاتهما في النمذجة بالترسيب المنصهر .(FDM) تم تصنيع خيوط مركبة تحتوي على نسب مختلفة من ألياف الكربون الدقيقة (MCF) لكلتا المصفوفتين، وتم دراسة خواصها الميكانيكية وامتصاص الرطوبة والخصائص المورفولوجية بشكل شامل.

أظهرت مركبات PP تحسنًا كبيرًا في مقاومة الشد والانحناء مع إضافةMCF ، حيث حققت أفضل تحسين عند نسبة 9.09% وزناً، بزيادة قدرها 75% و100% على التوالي مقارنة بـ PP النقي. في المقابل، أظهرت مركبات PLA زيادات طفيفة في القوة عند نسب منخفضة من MCF (أقل من 5%)، لكنها انخفضت مع زيادة محتوى الألياف عن هذا الحد.

كلا المادتين أظهرتا زيادة في الصلابة (معامل المرونة) مع ارتفاع مستوياتMCF ، مع تحقيق PLA أقصى قوة عند تحميل أقل للألياف. أما امتصاص الرطوبة فقد زاد في كلا المادتين مع زيادة محتوى الألياف؛ حيث أظهر PP زيادة متناسبة، بينما أظهر PLA امتصاصًا أكثر وضوحًا بسبب وجود المسام داخل وبين الخيوط.

سلط الفحص المجهري الضوئي (OM) الضوء على اختلافات إضافية: احتفظ PP بتوزيع الألياف والترابط على نطاق واسع من مستوياتMCF ، في حين أظهر PLA التصاقًا قويًا للألياف وسلوك كسر مرن عند مستويات منخفضة من MCF، متحولًا إلى كسر هش وتكوين مسام عند المستويات الأعلى.

أكدت نمذجة الانحدار باستخدام العمليات الغاوسية (GPR) هذه الاتجاهات، وحددت المحتوى الأمثل من MCF عند 9.09% وزناً لـ PP وحوالي 2.5% وزناً لـ .PLA تقدم هذه النتائج إرشادات لاختيار المواد وتحميل الألياف لتطبيقات FDM، حيث تحقق كل مادة توازنًا فريدًا بين الأداء الميكانيكي ومقاومة الرطوبة.